Materials and Methods

Extract preparation High speed Xenopus egg extracts were prepared as previously described with modifications of the centrifugation conditions (*S1*). Briefly, low speed CSF-arrested extracts were prepared by crushing dejellied Xenopus eggs in CSF-XB (10 mM K-HEPES, pH 7.7, at 16°C, 100 mM KCl, 2 mM $MgCl_2$, 50 mM sucrose, 5 mM EGTA) supplemented with protease inhibitors and 1mM DTT at 10,000g for 10 min at 4°C. Then, the low speed extracts were diluted 10-fold in the same buffer overlaid with mineral oil and then centrifuged at 200,000g for 1 h at 4°C to remove the internal membranes. The clear supernatant was reconcentrated to its original volume in Centriprep YM-10 concentrators (Milipore 4304). The usual final concentration is about 25 mg/ml. High speed extracts were supplemented with 200 mM sucrose and CSF-energy mix containing 1 mM ATP, 1 mM $MgCl_2$, and 7.5 mM creatine phosphate, snap frozen and stored at -80°C.

Plasmid construction In order to construct plasmids for fluorescent fusion proteins, we obtained Xenopus full-length Xenopus VASP clone from Open Biosystems. Mouse mDia2 plasmid was a gift from Arthur Alberts, human fascin plasmid from Danijella Vignjevic, and mCherry plasmid from Roger Tsien. Human Cdc42, toca-1 (*S2*), mouse mDia2, Xenopus VASP , and human fascin were subcloned into pCS2 vector with N-terminal hexahistadine tag and eGFP/mCherry. EcoR I and Xho I restricton sites were used for Cdc42, toca-1, VASP, and fascin, BspE I and Kpn I for mDia2, Bovine N-WASP was subcloned into pCS2 vector without tag using Fse I and Asc I restriction sites. Human WIP1 was subcloned into pCS2 vector with N-terminal zz-tag and TEV protease site. For the non-fluorescent version, human Cdc42 was

subcloned into pCS2 vector with N-terminal hexahistadine tag. Diaphanous interacting protein-LRR fragment (residues 507-722) was prepared by PCR using Human full-length DIP obtained from Open Biosystems and primers, gatcggatccatcctggccatggtcttctc and gatcctcgagctagctgggagcctccccca and subcloned into BamHI and Xho I sites of pGEX vector. This region does not contain the reported Arp2/3 complex activation sequence (*S3*). The GST-CA plasmid has been previously described (*S4*). GST-RhoA-N19 plasmid was a gift from Gary Bokoch (Addgene plasmid 12960). pEGFP GFP-PLCδ PH domain plasmid was a gift from Seth Field and was subcloned using EcoRI and NotI restriction sites into pGEX-4T2. RhoGDI plasmid for mammalian expression was a gift from Orion Weiner.

Protein purification and labeling N-WASP-WIP, toca-1, and Arp2/3 complex were purified as previously described (*S2*). Cdc42-RhoGDI, mCherry-Cdc42-RhoGDI, GFP-N-WASP-WIP, GFP/mCherry-toca-1, GFP-mDia2, GFP-VASP, and GFP-fascin were expressed in 293F cells using 293Fectin (Invitrogen) for 2 days. GFP/mCherry-toca-1 was purified in the same way as unlabeled toca-1. For the other proteins, the culture was resuspended in phosphate-buffered saline (PBS) with 0.5 mM DTT, protease inhibitor tablets (Roche), and 10 mM imidazole. For GFP-mDia2, 1% NP-40 was supplemented. For GFP-fascin, 0.5% Triton X-100 was supplemented. For GFP-N-WASP-WIP, it was in PBS with 1 mM DTT, protease inhibitor tablets.After the sonication, the lysate was cleared by centrifugation at 200,000g for 30 min at 4°C and incubated with Ni-NTA-agarose beads (Qiagen) for 2 hours at 4°C. For GFP-N-WASP-WIP, the cleared lysate was incubated with IgG sepharose beads (GE Healthcare) for 3 hours at 4°C. For the his-tagged GFP fusion proteins (GFP-mDia2, GFP-VASP, and GFP-fascin), the beads were washed with cold PBS with 0.5 mM DTT and 20 mM imidazole, eluted with 300

mM imidazole in PBS with 0.5 mM DTT, and dialyzed against XB (20 mM HEPES, pH 7.6, 100 mM KCl, 1 mM $MgCl_2$, 0.1 mM EDTA, 1 mM DTT) with 10 % Glycerol. For GFP-fascin, the dialysis was done against PBS supplemented 1 mM DTT and 10% Glycerol. For GFP-N-WASP-WIP, the beads were washed with cold PBS with 1mM DTT and incubated with 0.03mg/ml GST-TEV protease in the same buffer for 1 hour at room temperature, followed by removal of GST-TEV protease using glutathione-sepharose beads (GE Healthcare) and dialysis against XB with 10% Glycerol. pGEX GST-CA, RhoA-N19 vector were transformed into BL21 Codon Plus (DE-3)-RP (Stratagene). The bacteria were grown in LB media at 37°C until OD600 reached 0.6, then induced with 0.5mM IPTG and incubated at 24 °C overnight. The culture was resuspended in PBS with 1 mM DTT, protease inhibitor tablets (Roche), and 1 mg/ml lysozyme and incubated for 20 min on ice before sonication. The lysate was cleared by centrifugation and incubated with glutathione-sepharose beads (GE Healthcare) for 4 hours at 4 °C. The beads were washed with cold PBS with 1 mM DTT, eluted with 50 mM glutathione in PBS with 1 mM DTT, and dialyzed against XB with 10% Glycerol. GST-LRR and GST-GFP-PLCδ PH domain were transformed into the same BL21s, grown in TB media until log phase, induced with 0.5 mM IPTG and then incubated at 19 °C overnight. The purification was performed similarly to the other GST tagged proteins, except 150 mM NaCl, 20 mM HEPES pH 7.4, 2 mM EDTA and 2 mM DTT was used instead of PBS. In the case of RhoA-N19, all the buffers were supplemented with 1 mM $MgCl_2$. The labeling of Arp2/3 complex with Alexa568-maleimide (Invitrogen) has been previously described (*S5*). Alexa 488 or 647 labeled rabbit muscle actin was purchased from Invitrogen. All proteins were snap frozen and stored at -80 °C.

Liposome preparation Porcine brain PC, bovinc liver PI, porcine brain PS and porcine brain PI(4,5)P_2 were used for most experiments. Di-oleoyl phosphoinositides were used for the PIP specificity experiments and protonated before use by resuspension in chloroform:methanol: water 20:9:1, addition of water acidified with HCl to pH 2.5, and taking the lower chloroform layer. These lipids, rhodamine-PE and TopFluorPI(4,5)P_2 were purchased from Avanti Polar Lipids. Fluorescent lipids were used at 1%. To make liposomes, lipid mixtures were rapidly dried in glass tubes under a stream of dry nitrogen gas and further dried under vacuum for 1hr to remove chloroform completely. The dried lipid mixture was hydrated in XB buffer to a final concentration of 2 mM, bath sonicated for 1 min and then filtered using a mini-extruder sequentially through 800 nm then 100 nm pore-size polycarbonate membranes (Whatman). DiI (1,1'-dioctadecyl-3,3,3',3'-tetramethylindocarbocyanine perchlorate) was purchased from Invitrogen.

Antibody preparation To raise a *Xenopus* fascin antibody, the full-length Xenopus fascin clone was obtained from Open Biosystems and subcloned into the pGEX vector. Using BL21 as above, *Xenopus* fascin was expressed and purified as previously described (S6). Purified full-length Xenopus fascin was used to raise antisera in rabbits (Cocalico, Reamstown, PA). The antibodies were affinity purified using the same fascin proteins according to (*S7*). Drf1 and profilin antibodies were purchased from Axxora. The N-WASP antibody has been previously described (*S8*).

FLS assays To make the supported bilayers, No. 1.5 glass coverslips were incubated with freshly prepared liposomes containing 45 % PC, 45 % PI, and 10 % PI(4,5)P_2 in XB buffer for

20 min at room temperature, followed by extensive washing with XB buffer. Membrane phase separation was variable and was largely influenced by the particular batch of glass. Rigorous washing of the coverslips with hot detergent also promoted the liquid disordered phase. All assays were carried out at room temperature (~22 °C). For the purified system experiments, prenylated Cdc42.GTPγS was supplied to the lipid bilayer from 100 nM Cdc42-RhoGDI in solution using the EDTA exchange reaction (*S9*). The reaction mixture including N-WASP-WIP, toca-1, Arp2/3 complex, and actin as previously described (*S2*) was added after Cdc42 loading. Typical FLS reactions (50 µl volume) contained a 2-fold dilution of *Xenopus* egg extract, 4 µM Alexa 647 actin (10% labeling efficiency, rabbit skeleton muscle actin), 0.35 M sucrose, 1 mM ATP, 1 mM $MgCl_2$, 7.5 mM phosphocreatine in XB buffer. The reaction mixtures were added on top of the freshly prepared supported bilayer and monitored with a spinning disk confocal microscope. For the pulse chase experiments, the second reaction (5 µl volume) Xenopus egg extract, 12 µM Alexa-488 actin (5% labeling efficiency, rabbit skeletal muscle actin), 1 mM ATP, 7.5 mM phosphocreatine in XB and 5 µl was added gently on top of the first reactions. For dose response of FLS initial elongation, the reaction mixture was supplement with different dose of GST-CA and images were taken after 7 min. For Arp2/3 complex independent elongation experiments, the first reaction was supplemented with 50 nM Alexa568-Arp2/3 complex. The second reaction is assembled similarly to the pulse-chase experiments with different doses of GST-CA. For the GFP-PH domain experiments, 50-300 nM was used. For timelapse movies of FLS growth, an oxygen scavenger mix was added which contained: 4.5 mg/ml glucose, 0.5 % 2-mercaptoethanol, 0.2 mg/ml glucose oxidase (Sigma-Aldrich), 35 µg/ml catalase (Sigma-Aldrich).

Light microscopy Microscopy for figures 1, 2 and 5 was performed using an inverted Nikon TE2000U microscope with a 100x, 1.4 NA Plan Apochromat objective lens and motorized stage and focus motor from Prior. Confocal images were obtained using a Yokogawa CSU-10 spinning disk confocal head with Prairie laser launch with a 2.5 W water-cooled Coherent Argon-Krypton laser. Excitation and emission wavelengths were selected and attenuated with an AOTF and a triple 488/568/647 dichroic mirror from Chroma. GFP and Alexa-488 were visualized using the 488 laser line and 525/50 emission filter; Alexa-568 was visualized using the 568 laser line and 600/45 emission filter; Alexa-647 was visualized by the 647 laser line and 700/75 emission filter (Chroma). Images were collected with a ORCA-AG cooled CCD camera from Hamamatsu and Metamorph software v7.6 (Molecular Devices). Exposure times were typically 100~400 ms using 25~50% laser power and a bin of 2x2. Z-stacks were collected with a step size of 0.5 µm. Light microscopy for figure 3 and supplementary figures 2, 3 and 4 was performed using an inverted Nikon Ti-E microscope with a 100x, 1.4 NA Plan Apochromat objective lens and motorized stage from Prior. Confocal images were obtained using a Yokogawa CSU-10 spinning disk confocal head with 100 mW Argon-Krypton laser from Melles Griot. Excitation and emission wavelengths were selected using Sutter filter wheels and a triple 488/568/647 dichroic mirror from Chroma. Images were collected with an ORCA-ER cooled CCD camera from Hamamatsu and Metamorph software v7.6 (Molecular Devices). GFP was visualized using the 488 laser line selected with a 488/10 excitation filter and 525/50 emission filter; rhodamine and Alexa-568 were visualized using the 568 laser line selected with a 568/10 excitation filter and 620/60 emission filter; Alexa-647 was visualized by the 647 laser line selected with a 647/10 filter, and 647/10 emission filter (Chroma). Exposure times were typically 200 ms using a bin of 2x2. For time-lapse experiments of FLS initiation, the Perfect

Focus System (Nikon) was used to maintain focus, and images were acquired every 10 s for 10 minutes. Z-stacks were acquired with a step size of 1 μm. For the fluorescence recovery after photobleaching experiments of the supported bilayer, wide-field epifluorescence illumination was used (with a Hamamatsu ORCA-R2 cooled CCD camera and an X-Cite series 120 light source) and

rhodamine-PE was photobleached to 80-90% of initial intensity with 515 nm light from a nitrogen pulse laser (Photonic Instruments Micropoint system) focused to a spot less than 1 micron in diameter. The filter was Y-2E/C (excitation: 560/40 dichroic: 595 emission; 630/60) from Nikon. The exposure time was 25 ms, and images were typically acquired every 1 s for 1-20 min. For the multispectral total internal reflection fluorescence microscopy in figure 4, we used a Nikon Ti-E inverted motorized microscope with integrated Perfect Focus System, Nikon 100x 1.49 NA TIRF DIC objective lens, Nikon halogen trans illuminator with 0.52 NA LWD and 0.85 NA Dry condenser, Nikon dual-port TIRF/Epi illuminator with motorized laser incident angle adjustment and motorized switching between TIRF and epi-illumination. For lasers, a Solamere laser launch was used with 100mW 491nm, 75mW 561nm and 30mW 640nm solid state lasers with a fiber-optic delivery system and 4-channel AOTF. A Prior Proscan II controller was used for fast excitation and emission filter wheels, fast transmitted and epi-fluorescence light path shutters, and a linear-encoded motorized stage. A Chroma zet405/491/561/638 dichroic mirror was used with a 491 nm laser line and a 525/50 emission filter for GFP; a 561 laser line and 600/50 emission filter for Alexa568; and a 640 laser line and a 700/75 emission filter for Alexa647. In addition to emission filters, a custom Chroma laser notch filter was used in the emission path to further block the illumination light from reaching the camera and to minimize interference patterns. Images were collected with a Hamamatsu ImagEM 512x512 back-thinned

electron multiplying cooled CCD camera and MetaMorph v7.7 (Molecular Devices). Exposure times were typically ~100 ms using 25~50% laser power.

Electron microscopy To observe the ultrastructure of the FLSs by electron microscopy, we use a protocol which minimizes convection, and allows extraction of soluble proteins without fragmenting the FLSs. This problem is not usually encountered fixing intact cells but because the FLSs only have a small point of adherence to the glass and do not have surrounding membrane, they are vulnerable to pipetting. In order to prevent the fragmentation of FLSs from the convective flow, it is important to add sufficient amount of sucrose to the reactions and add stabilization solution on top of the reaction very gently and let it diffuse into the reaction. Typically 11 % (w/v) sucrose is included in the reaction FLSs are stabilized and arrested by the incubation with 20μM each of phalloidin and latrunculin B for 1 min (*S10*), followed by repeated gentle dilution using XB buffer to remove soluble proteins and then fixed with 0.1% glutaraldehyde in XB for 20min. Use of negative stain to visualize actin structures has been described previously (*S11*). Briefly, fixed FLSs were rinsed three times in XB, and the actin filaments were further stabilized by incubation in 10 μg/ml phalloidin in the same buffer for at least 20 min or until use. To detach FLSs, the glass surface was scratched using a scalpel or a pipet tip. The detached FLS were adsorbed onto glow-discharged formvar-carbon coated grids, and negatively stained with aqueous 3 % sodium silico-tungstate. The electron microscope was a Tecnai G² Spirit BioTWIN electron microscope operating at 80 kV. For unfixed FLSs, they were first stabilized and arrested by 20 μM each of phalloidin and latrunculin B for 1 min. Then, soluble proteins were removed by repeated gentle dilution with XB. These FLSs were easily

detached from the lipid bilayer by pipetting for the same negative staining. Alternative buffer conditions or additives for FLS fixation are also described elsewhere (*S11*, *S12*).

Immunostaining FLSs were fixed using 4 % formaldehyde in CB for 40 min. It is important to add the fixation mixture very gently on the reactions. Typically, 200 µl of the fixation solution was added to a 50 µl reaction. 2 % BSA was used for blocking, the FLSs were incubated with primary antibody or anti-serum (1:100 dilution), followed by incubation with Alexa 488-conjugated goat anti-rabbit secondary antibody (1:200 dilution) (Invitrogen). After extensive washing, actin was stained with Alexa-568 conjugated phalloidin (Invitrogen).

Immunodepletion Immunodepletion of N-WASP and toca-1 from *Xenopus* egg extracts is described elsewhere (*S1*).

Image Analysis Image analysis was performed using MetaMorph (Molecular Devices). FLS elongation was measured using reconstructed side view images. The linescan method in MetaMorph was used measure actin fluorescence intensity along the tails. In the cases of pulse chase and Arp2/3 complex independent elongation experiments, the second actin signals were divided by the first actin signals along the FLS tail lengths. The elongation of the second color of actin was measured at the point it disappeared. We sampled 10~20 FLSs per field of view at each time point to calculate mean and standard deviation of elongations. The standard deviation of elongation rate between time t_1 and t_2 is calculated as $\sqrt{\sigma_2^2 + \sigma_1^2} \big/ (t_2 - t_1)$ where σ_1 and σ_2 are the standard deviations of FLS elongation at time t_1 and t_2 under the assumption that the

measurements at t_1 and t_2 are statistically independent. For quantitation of Alexa568-Arp2/3 complex in Arp2/3 complex independent elongation experiments, the fluorescence at 1μm from bilayers was measured from reconstructed side view images of Arp2/3 complex and was subtracted by the nearby background fluorescence. For quantitation of the density and rate of appearance of FLS nuclei, the Transfluor quantitation tool of MetaMorph was used . The typical parameter values of the analysis were a threshold of 200 intensity values and a size range of 0.5-10 μm. In order to quantify the diameter of FLSs, we used Cell Scoring tool of Metamorph for segmentation and the cross-sectional are of FLSs were measured using Morphometry Analysis tool. Then, the effective diameters of FLSs were calculated as $2\sqrt{A/\pi}$ where A is a FLS cross-sectional area. For the fluorescent protein recruitment experiments, FLSs were identified at the end of the time-lapse sequence and by back-tracking and observation by eye, the first frame where the fluorescence for actin and the candidate protein is higher than background was noted. We have normalized the recruitment time of each component to the recruitment time of labeled actin. We find that this is a more informative way to quantify the kinetic data than, for example, the time of half-maximal accumulation. The latter is biased by the largest structures, is more sensitive to photobleaching and conflates the time of recruitment with the extent of assembly. The website www.physics.csbsju.edu/stats was used for ANOVA, KS and t-tests. Microsoft Excel was used to make the graphs and contour plot. AutoQuant was used to make the 3D reconstruction image of FLSs.

Supporting Videos 1-4 Time-lapse videos showing growth of FLSs in z-stack reconstructions. Video 1 shows z-stack reconstruction viewing in x-y of a large field of view. Video 2 shows the same reconstruction viewing in z-x. Video 3 is a close-up of a small area in x-y. Video 4 is a close-up of a small area in z-x. Experimental duration: 14 mins. Movies are speeded up 280x.

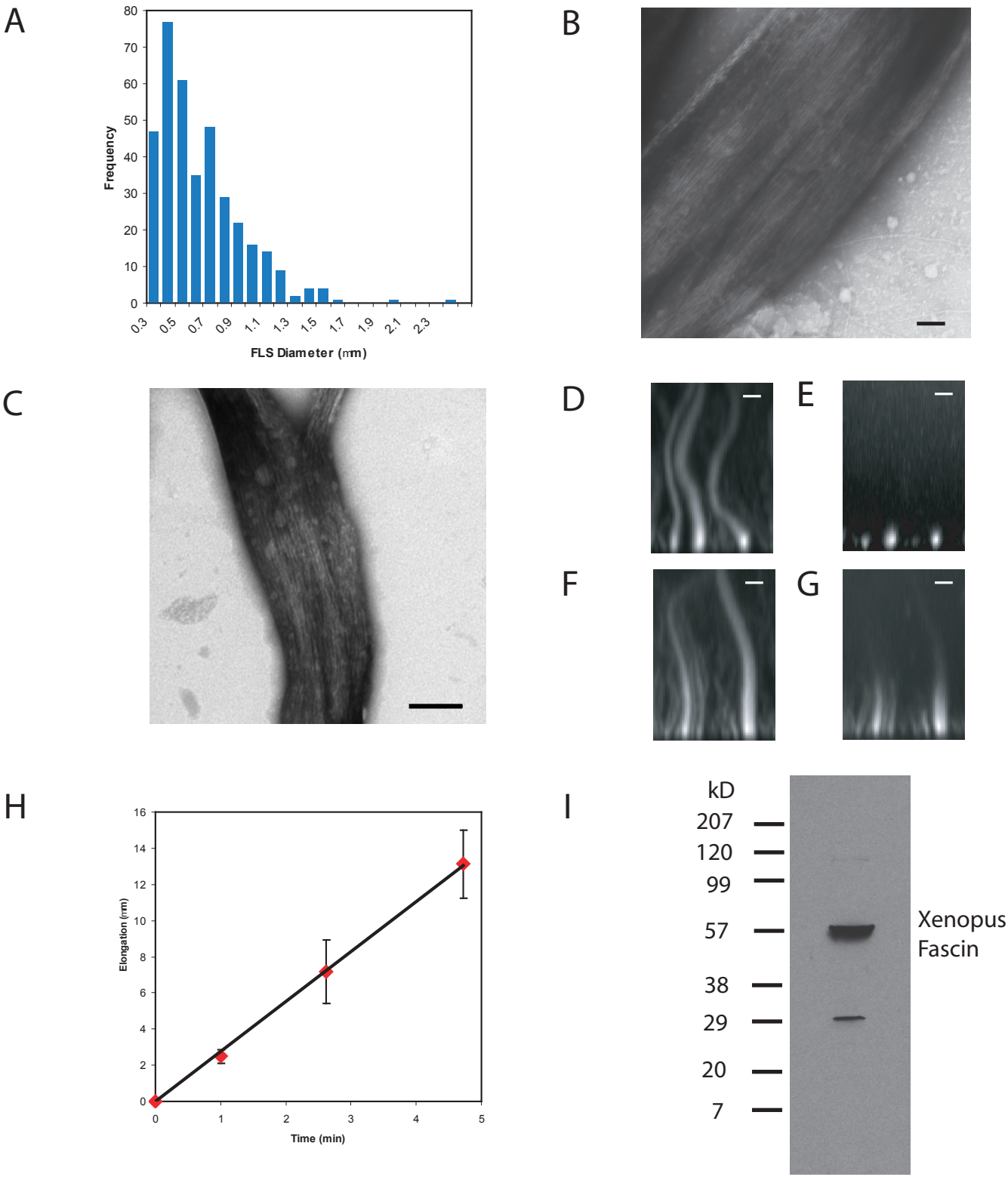
A
Frequency
FLS Diameter (mm)
B
C
D
E
F
G
H
Elongation (nm)
Time (min)
I
kD
207
120
99
57
38
29
20
7
Xenopus
Fascin

Figure S1

Figure S1 FLS diameter histogram, electron microscopy and quantitation of pulse chase elongation rate The lipid composition used was 45% PC, 45% PI, 10% PI(4,5)P_2 (A) The distribution of FLS diameters. Due to the diffraction limit, the value for the 0.3 μm bin includes all FLSs whose diameters are below 0.3 μm. (B) Negative-stain electron microscopy of the phalloidin-stabilized actin structures shows actin bundles of typical FLS size. Bars: 100 nm (C) Negative-stain electron microscopy of the glutaraldehyde-fixed actin structures shows similar actin bundles to the unfixed samples. Bar: 100nm (D) First color actin (red) and (E) Second color actin (green) in Figure 1I. (F) First color actin (red) and (G) Second color actin (green) in Figure 1J. Bars: 2 μm. (H) The elongation curve for the second color of actin in pulse chase experiments. The linear fitting line shows the elongation rate is 2.8 μm/min. Error bars are s.d. (I) Western blot of *Xenopus* extract using the rabbit polyclonal antibody raised and affinity purified against *Xenopus* fascin.

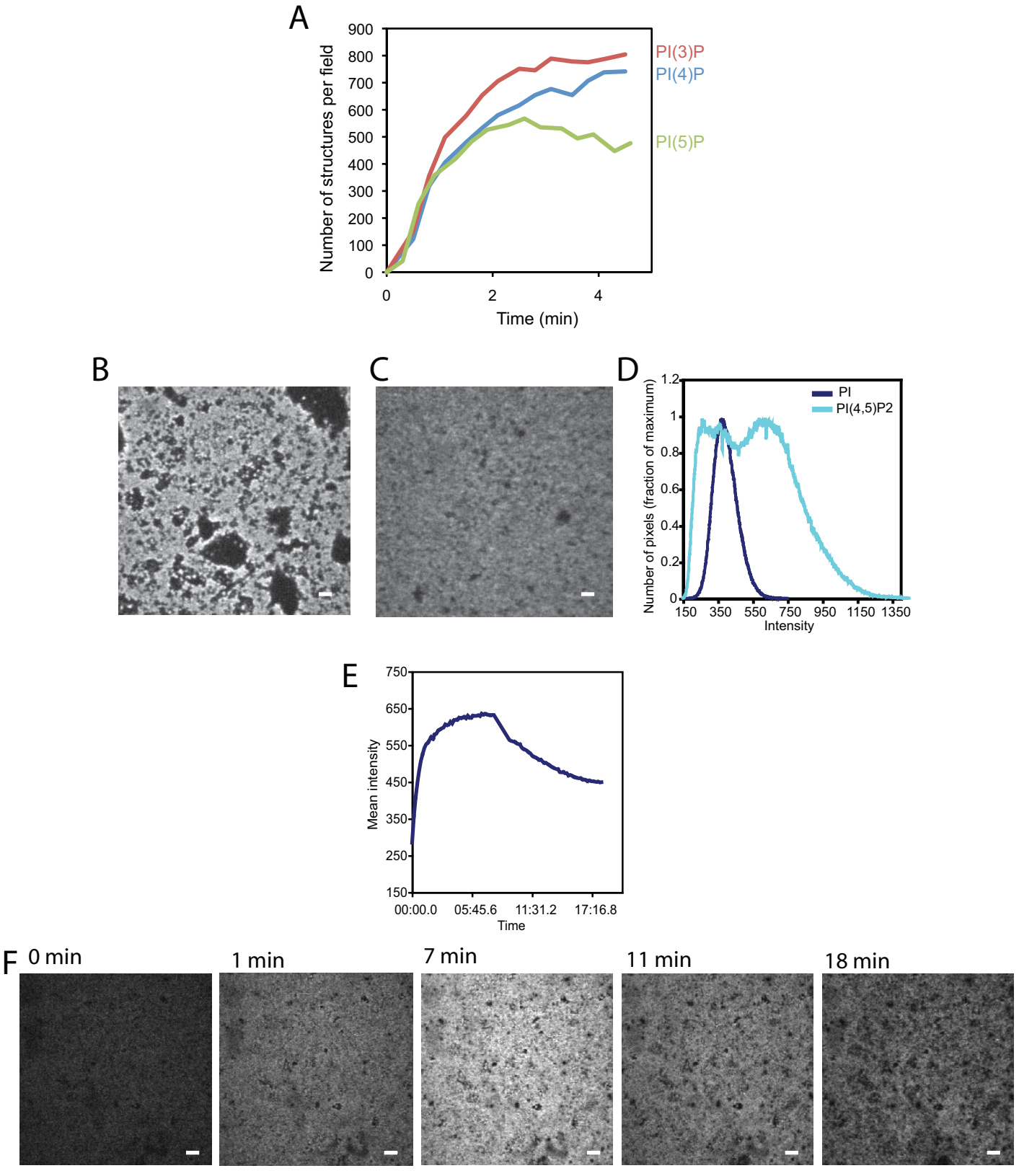
A
Number of structures per field
900
800
700
600
500
400
300
200
100
0
0
2
4
Time (min)
PI(3)P
PI(4)P
PI(5)P
B
C
D
Number of pixels (fraction of maximum)
1.2
1
0.8
0.6
0.4
0.2
0
150 350 550 750 950 1150 1350
Intensity
PI
PI(4,5)P2
E
Mean intensity
750
650
550
450
350
250
150
00:00.0 05:45.6 11:31.2 17:16.8
Time
F
0 min
1 min
7 min
11 min
18 min

Figure S2

Figure S2 Control experiments for GFP-PLCδ PH domain binding to the supported bilayer. (A) Time course of actin spot appearance with monophosphorylated PIPs. Compositions: 60% PC/30% PS/10% PIP, where pink:PI(3)P, blue:PI(4)P green:PI(5)P. Data are the mean of 3 timecourses normalized to the average number of structures per experiment. Most monophosphorylated PIP actin spots fail to elongate. (B) 50 nM GFP-PLCδ PH domain binding to supported bilayer made from liposomes containing 45% PC, 45% PI, 10% $PI(4,5)P_2$. (C) 50 nM GFP PLCδ PH domain binding to supported bilayer made from liposomes containing 50% PC, 50% PI. (D) Image intensity histogram of PI and $PI(4,5)P_2$ bilayers. (E) Kinetics of GFP-PLCδ PH domain binding to $PI(4,5)P_2$ supported bilayer and dissociation after washing. (F) Time-lapse pictures of GFP-PLCδ PH domain binding to $PI(4,5)P_2$ supported bilayer from the graph shown in (E) show that no $PI(4,5)P_2$ punctae are revealed by kinetic analysis. All bars: 2 μm. Similar characteristics of GFP-PH domain binding was observed for 60% PC/30% PS/10% $PI(4,5)P_2$, and background binding similar to PI was observed for the other bisphosphorylated phosphoinositides, confirming the specificity of the domain.

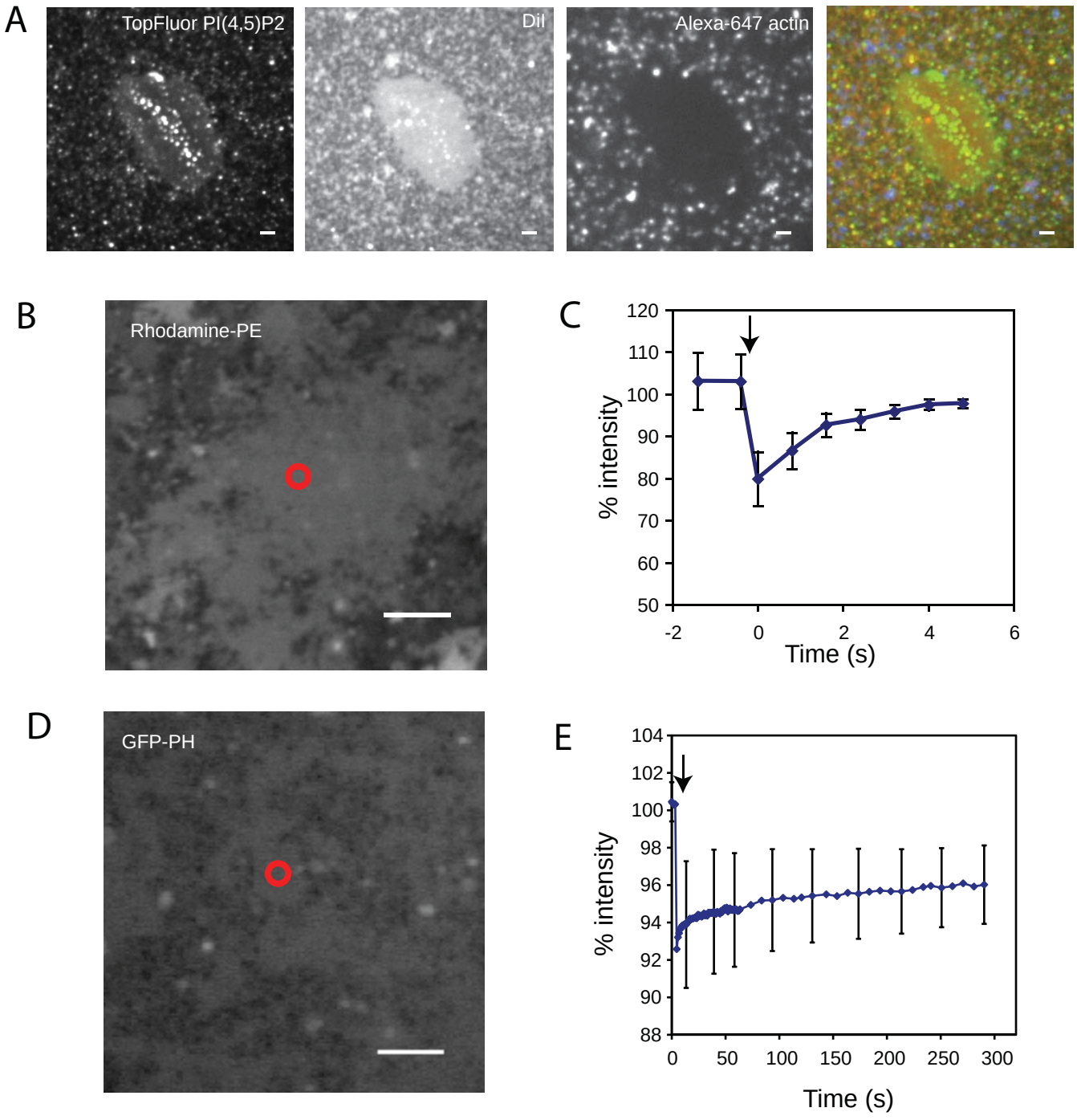
A
TopFluor PI(4,5)P2
DiI
Alexa-647 actin
B
Rhodamine-PE
C
% intensity
Time (s)
D
GFP-PH
E
% intensity
Time (s)

Figure S3

Figure S3 Domain formation and FLS distribution in supported bilayers. (A) Additional fluorescent markers that partition into the liquid disordered phase and thus do not label areas where FLSs grow: TopFluor PI(4,5)P_2 (green) and DiI (red). Shown with actin structures (blue). The TopFluor fluorescent moiety on the sn-2 position of TopFluor PI(4,5)P_2 is structurally very different from an arachidonyl chain and by comparison with Fig. 2D, it is evident that TopFluor PI(4,5)P_2 partitions differently from natural PI(4,5)P_2. (B,C) Rhodamine-PE is fluid within enriched areas. Fluorescence recovery after photobleaching experiment showing example image in (B) and quantitation of five independent experiments in (C). Error bars are s.d. (D,E) Fluorescence recovery after photobleaching experiment of GFP-PH domain showing the much slower recovery compared with rhodamine-PE, confirming that this domain binds PI(4,5)P_2 that is within the gel phase. Error bars are s.d. All bars: 2 μm. The lipid composition used was 45% PC, 45% PI, 10% PI(4,5)P_2. The partitioning and fluidity of rhodamine-PE was tested and found to be similar for all lipid compositions described in the paper.

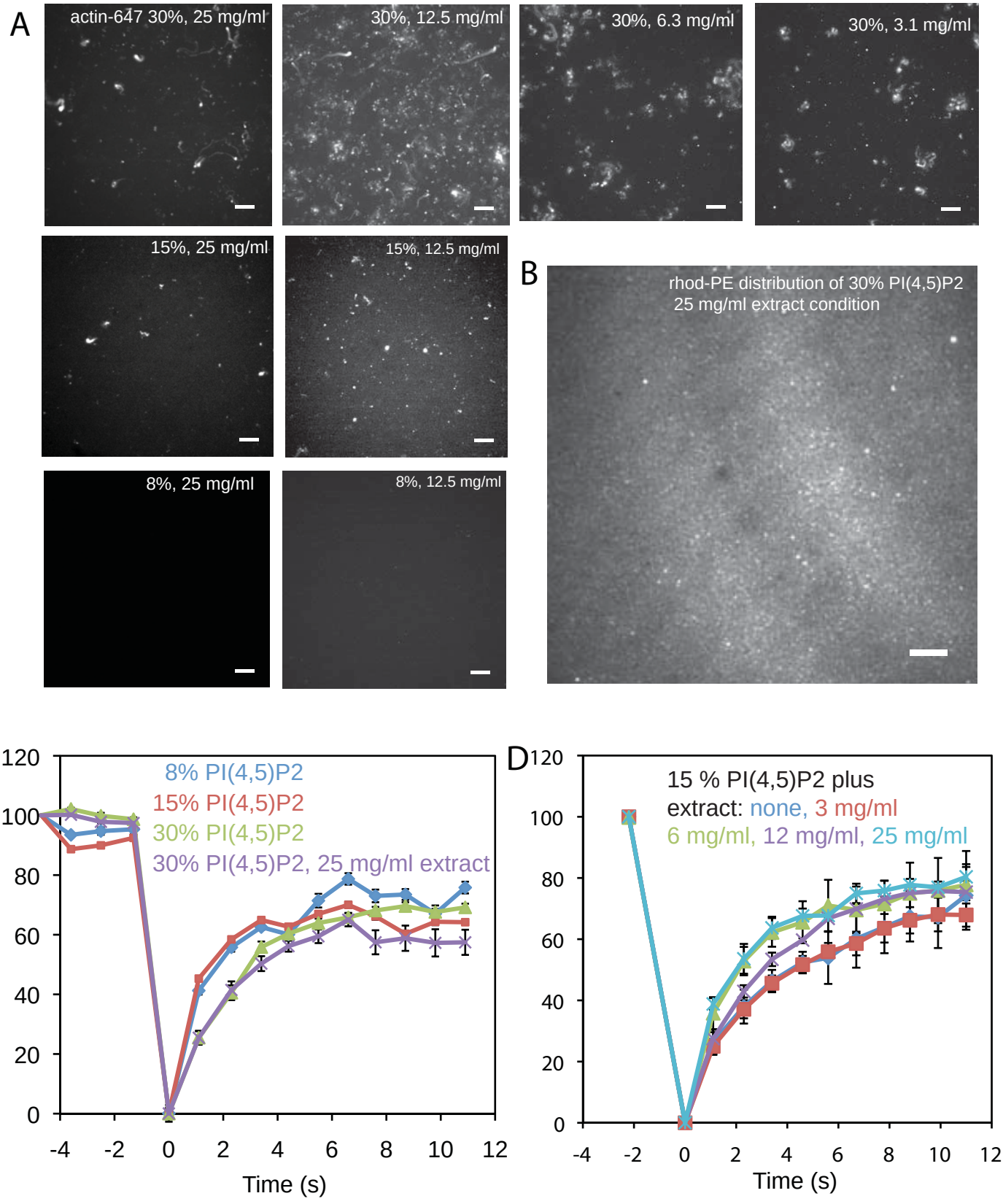
A
actin-647 30%, 25 mg/ml
30%, 12.5 mg/ml
30%, 6.3 mg/ml
30%, 3.1 mg/ml
15%, 25 mg/ml
15%, 12.5 mg/ml
8%, 25 mg/ml
8%, 12.5 mg/ml
B
rhod-PE distribution of 30% PI(4,5)P2
25 mg/ml extract condition
C
Normalized intensity (%)
Time (s)
8% PI(4,5)P2
15% PI(4,5)P2
30% PI(4,5)P2
30% PI(4,5)P2, 25 mg/ml extract
D
Time (s)
15 % PI(4,5)P2 plus
extract: none, 3 mg/ml
6 mg/ml, 12 mg/ml, 25 mg/ml

Figure S4

Figure S4 Rescue of FLS formation from fluid membranes by increased PI(4,5)P_2 and extract concentrations. (A) Single representative compressed z-stacks shown in x-y orientation for data the quantified in Fig. 2F. The quantification was an average of ~10 images from each using 8, 15, 30 % PI(4,5)P_2 by mols with background lipid composition of 45% PC and pro-rated mol fraction PI. Each condition was tested with 3.1, 6.3, 12.5 and 25 mg/ml extract concentration. Increasing the mol fraction of PI(4,5)P_2 and the extract concentration rescues FLS formation from fluid membranes. No structures are seen for 15% PI(4,5)P_2 at less than 12.5 mg/ml extract concentration. (B) Supported bilayer from the 30% PI(4,5)P_2, 25 mg/ml extract condition as an example, showing the distribution of rhodamine-PE. (C) FRAP experiments of rhodamine PE at the different PI(4,5)P_2 concentrations with buffer or 25 mg/ml extract, as annotated showing that it remains unaltered. Data are the mean of 5 experiments, error bars are the standard deviation. To allow comparisons between the conditions, the initial intensity levels were normalized (to 100%) and the bleached intensity level, which was ~80-90% of initital intensity, normalized to 0%. (D) FRAP experiments of rhodamine-PE at increasing extract concentrations at 10% PI(4,5)P_2, again showing that rhodamine-PE fluidity remains unchanged. However we would expect that protein binding to the membrane will change the mobilities of some lipids and proteins: there will be no protein ligand for rhodamine within the frog egg extract, unlike with natural lipids. Data are the mean of 5 experiments, error bars are the standard deviation. To allow comparisons between the conditions, the initial intensity levels were normalized (to 100%) and the bleached intensity level, which was ~80-90% of initital intensity, normalized to 0%. Bars: 5 μm.

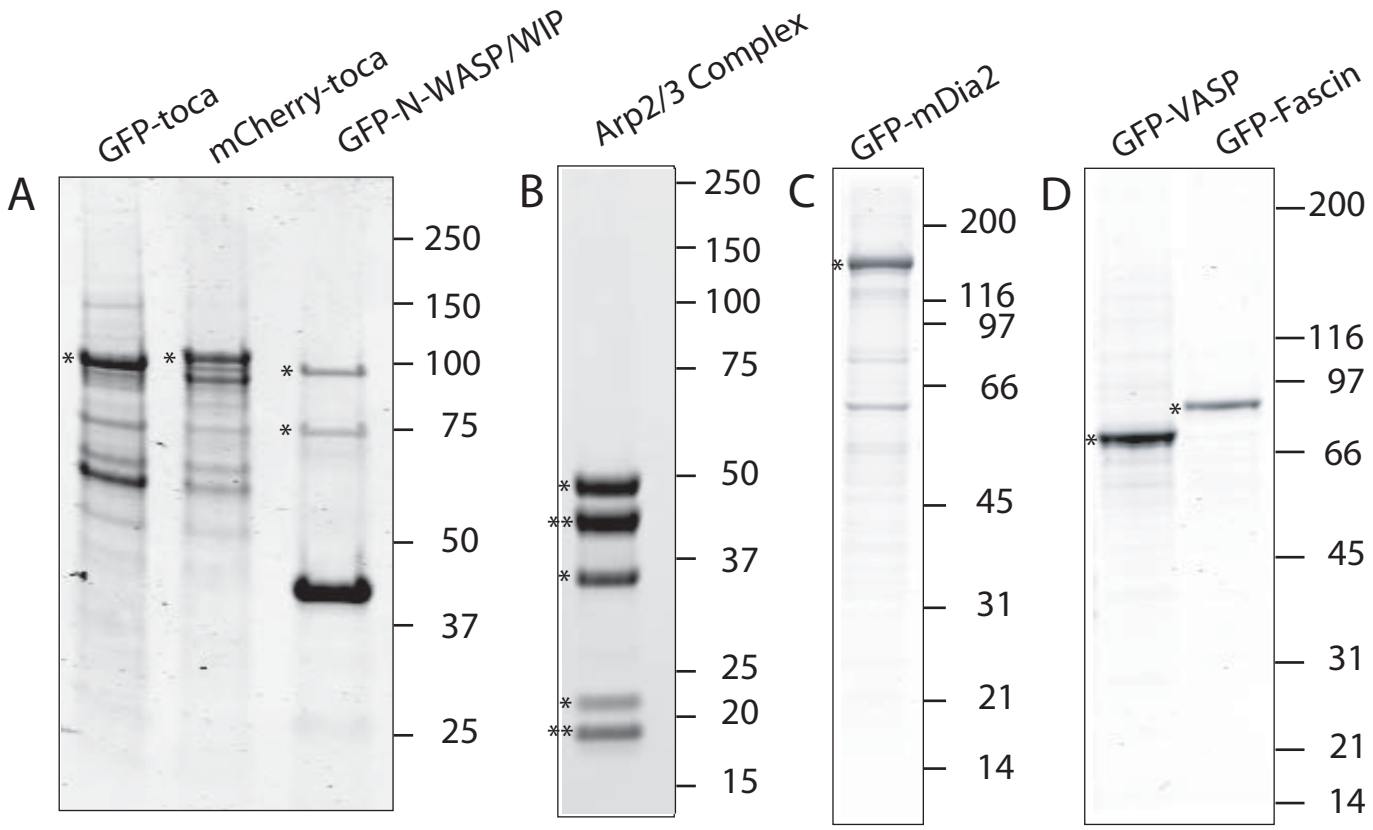

Figure S5 SDS-PAGE of the purified fluorescently tagged proteins. The tagged protein is labeled with an asterisk. (A) N-terminally his and GFP or mCherry toca-1, expressed in 293F cells and purified using Ni-NTA agarose, washing and elution with imidazole. N-terminally GFP-tagged N-WASP was purified as N-WASP/WIP complex using co-expression of ZZ-tagged WIP and IgG sepharose. The abundant band at 40 kDa is actin. (B) Purified Arp2/3 complex. Double asterisk indicates subunits that have similar mobility on this gel (4-12% gradient) (C,D) His-GFP-mDia2, his-GFP VASP and his-GFP fascin were expressed and purified similarly to toca-1.

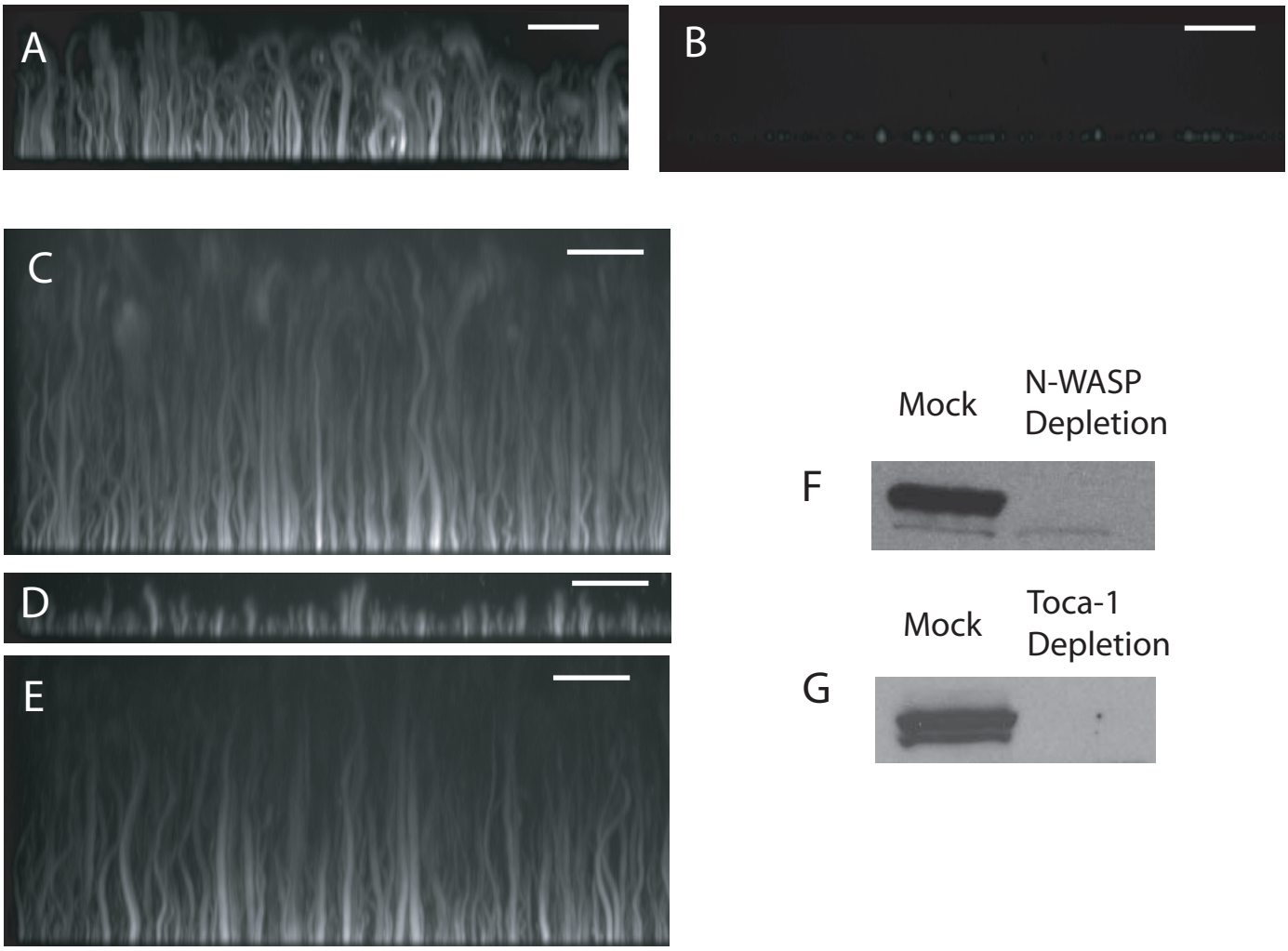
A
B
C
D
E
Mock
N-WASP Depletion
F
Mock
Toca-1 Depletion
G
H
Number of Focal Structures per Field
800
700
600
500
400
300
200
100
0
*
Mock
N-WASP
Toca-1
I
FLS Length (nm)
45
40
35
30
25
20
15
10
5
0
* *
*
Mock
N-WASP
Toca-1

Figure S6

Figure S6 The effects of GST-CA and immunodepletion of N-WASP and toca-1 on FLSs. The side view of FLSs at 7 min with 0 μM (A) and 40μM (B) GST-CA. The side view of FLSs at 20 min with (C) mock (rabbit IgG), (D) N-WASP (E) toca-1 depletion. Bars: 10 μm. (F-G) Western blots of depletions. (H) The number of focal actin structures after depletion (n=5), *p = 0.008. (I) The length of FLSs with depleted extracts (n=10), *p < 0.001, **p = 0.001. All error bars are s.d. In this experiment the lipid composition was 45% PC, 45% PI, 10% PI(4,5)P_2; similar results are obtained with 60% PC, 30% PS and 10% PI(4,5)P_2.

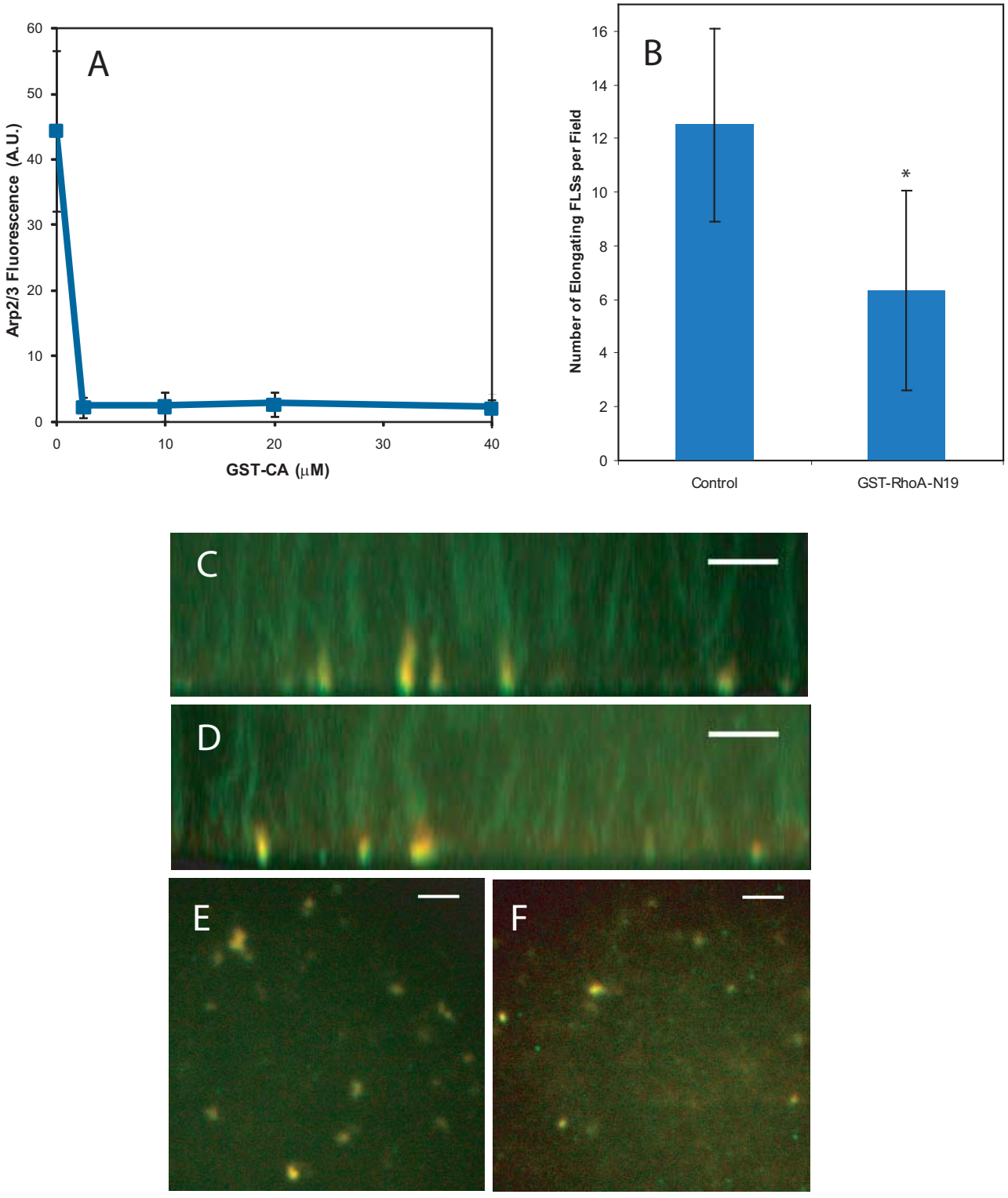
A
Arp2/3 Fluorescence (A.U.)
GST-CA (μM)
B
Number of Elongating FLSs per Field
Control
GST-RhoA-N19
*
C
D
E
F

Figure S7

Figure S7 (A) Quantification of the Arp2/3 complex fluorescence of the GST-CA inhibition experiment from Fig. 4G-H. The fluorescence of Alexa568-Arp2/3 complex in the FLS shafts was measured 1μm from the bilayer and is eliminated by GST-CA (n=15). **(B-F) Inhibition of FLS Arp2/3 complex independent elongation by dominant-negative RhoA.** The number of FLSs with Arp2/3 complex-independent elongation was reduced in the presence of 4 μM GST-RhoA-N19, similarly to our findings with GST-LRR (Fig. 4I-M). (B) Quantification of GST-RhoA-N19 addition (n=6), *p = 0.016. Side views of first actin in green and second in red for (C) control and (D) GST-RhoA-N19 addition. Actin on the bilayer, first in green and second in red for (E) control and (F) GST-RhoA-N19 addition. Bars: 5 μm. All error bars are s.d. The lipid composition was 45% PC, 45% PI, 10% PI(4,5)P_2.

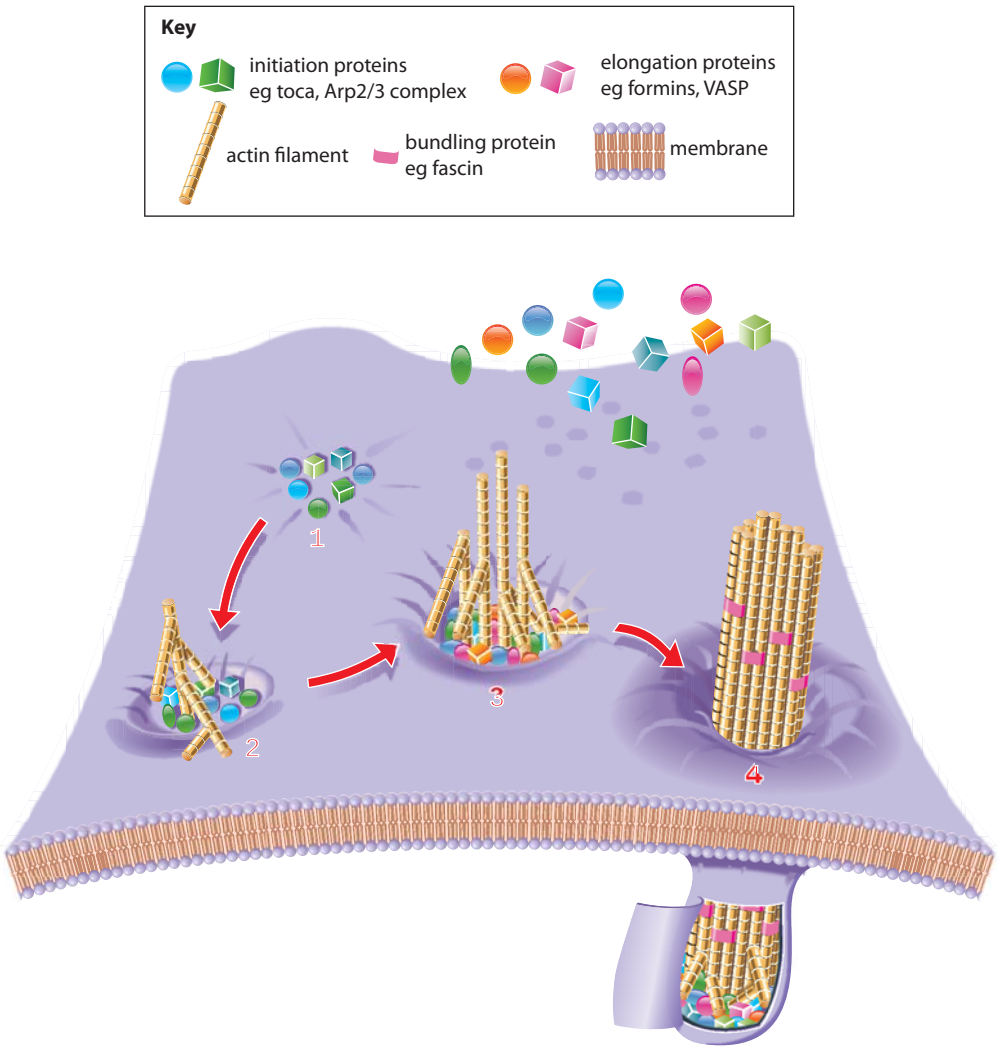

Figure S8 A clustering-outgrowth model for filopodia formation. Stage 1: symmetry-breaking via BAR domain proteins and stage 2: initial actin polymerization via N-WASP and Arp2/3 complex, indicated by blue/green shapes. Stage 3: recruitment of elongation factors and stage 4: bundling proteins, indicated by orange/pink shapes. The result is focal actin protrusion, characteristic of filopodia.

Supporting References

S1. Lebensohn, AM, Ma L, Ho HH, and Kirschner MW. Cdc42 and PI(4,5)P_2 - Induced actin assembly in Xenopus egg extracts, Methods in Enzymology, 406:146 (2006)

S2. Ho HY, Rohatgi R, Lebensohn AM, Kirschner MW. *In vitro* reconstitution of cdc42-mediated actin assembly using purified components. Methods Enzymol. 406:174 (2006)

S3. Kim DJ, Kim SH, Lim CS, Choi KY, Park CS, Sung BH, Yeo MG, Chang S, Kim JK, Song WK. Interaction of SPIN90 with the Arp2/3 complex mediates lamellipodia and actin comet tail formation. J Biol Chem. 281: 617 (2006)

S4. Miki, H., Miura, K., and Takenawa, T. N-WASP, a novel actindepolymerizing protein, regulates the cortical cytoskeletal rearrangement in a PIP2-dependent manner downstream of tyrosine kinases. EMBO J. 15, 5326 (1996)

S5. Zalevsky J, Grigorova I, Mullins RD. Activation of the Arp2/3 complex by the Listeria acta protein. Acta binds two actin monomers and three subunits of the Arp2/3 complex. J Biol Chem. 276:3468 (2001)

S6. Vignjevic D, Peloquin J, Borisy GG. In vitro assembly of filopodia-like bundles. Methods Enzymol. 406:727 (2006)

S7. Harlow, E and Lane D, Using Antibodies: A Laboratory Manual, Cold Spring Harbor Laboratory Press, Cold Spring Harbor, NY (1999)

S8. Rohatgi R, Ma L, Miki H, Lopez M, Kirchhausen T, Takenawa T, Kirschner MW. The interaction between N-WASP and the Arp2/3 complex links Cdc42-dependent signals to actin assembly. Cell. 97:221-31 (1999)